Sparse and Incomplete Signal Dictionaries for Reconstruction of MR Images

Original Scientific Paper

Deepak M Devendrappa
Department of CSE, K S School of Engineering and Management, Bengaluru.
Affiliated to Visvesvaraya Technological University, Gnana Sangama, Belagavi, India
deepak.m.d@kssem.edu.in

Karthik Pilani
Department of ECE, K S School of Engineering and Management,
Bengaluru, India.
karthik.p@kssem.edu.in

Deepak N Ananth
Department of CSE, R V Institute of Technology and Management,
Bengaluru, India
deepak.n.ananth@gmail.com

Abstract *– Compressed Sensing(CS) is a mathematical approach for data acquisition in which the signals are compressible and sparse w.r.t. to an orthonormal basis. These sparse signals are reconstructed from very less measurements. CS technique Is widely used in Magnetic Resonance Imaging (MRI) where the doctors suggest the patients to undergo MRI scans for diagnosing their body parts. During the prolonged MRI Scan, the exact slice of the MRI cannot be achieved due to the difficulties faced by the patient or irregular changes in the body position of the patient. The idea is to reduce the exposure time of the patient's body against the MRI scan by considering only fewer samples. Is it possible to Reconstruct the signal by making use of a fewer number of samples that are less than the Nyquist rate? Yes, it is possible to reconstruct the signal by making use of the Compressed Sensing or sampling Technique. Compressed sensing is a new framework for signal acquisition and representation in a compressible manner less below the Nyquist sampling rate. In this article, Sampling and reconstruction are dealt here thoroughly as part of the research activity. Compressive Sensing Matching pursuit (CoSaMP) is a novel technique for optimization. It is an iterative approximation method for sparse and incomplete signal recovery. CoSaMP method along with Different transform techniques is used for reconstruction. The FFT_CoSaMP, DCT_CoSaMP and DWT_CoSaMP are proposed methods for MR Image Reconstruction, where DWT-based CoSaMP along with different wavelet families give the best results when compared to other CS-based techniques w.r.t. PSNR, SSIM and RMSE analysis.*

Keywords*: Compressed Sensing, MRI, Nyquist Rate, CoSaMP, Dictionary learning*

1. INTRODUCTION

Compressed sensing (CS) [1] has become an interesting topic in these days for research in the field of mathematical, statistical, electrical and computer sciences, and engineering [2-5]. CS works on the basic fact that signals are represented by using a few non-zero coefficients in an appropriate dictionary or basis. As all of us know to capture a two-dimensional raw image of 256 X 256 size, each pixel will take around 8 bits of storage, the amount of storage required is 256 X 256 X 3 X 8, i.e., approximately, 1.5 Mb of memory. But as we observed, the image is stored in terms of KB. The reason is that image is stored in the compressed form only in terms of 15kb or 50 kb size approximately for example. When you try to open the image, the image is getting reconstructed by making use of some reconstruction algorithms. So that it is possible to look into the image in its original reconstructed form. The idea here is to minimize the number of sensors that are necessary to capture the raw image since the raw image is going to be compressed in its storage level. The notion behind the reduction of the number of sensors is to choose a less quantity of samples during the image acquisition. The number of samples captured violates the Nyquist theorem [11,32]. The Nyquist rate says that the sampling rate must be at least a minimum of two times the maximum frequency of the signal for the exact recovery of the signal. In contrary to this, the CS technique samples the signal at a level far lesser

than the Nyquist rate and it can be restored with high possibility. To compress the signal during the acquisition is the idea behind the compressed sensing and the compressed signal is reconstructed by making use of CS techniques.

Compression techniques which aim to get the concise representation of a signal with tolerable distortion. Some of the signal compression techniques are JPEG, MP3, JPEG2000, MPEG. In all these techniques, the whole signal is captured and duplicate signal data is removed stage by stage.

Donoho [4] challenged the traditional method of acquiring the whole signal and compressing it. He footed his first step into the area of Compressed Sensing or Compressive Sampling (CS). CS is a technique of reconstructing signals well from a fixed set of far fewer non-linear measurements bearing some incoherent characteristics [5,6,7]. Many real-time signals are characterized as sparse in some transforming domains like FFT, DCT, DWT. Since sparse signals exhibit very few non-zero coefficients, they can be represented by some linear measures. Non-linear approximations can approximate the recovery of such signals from a very less number of coefficients. Hence compressed sensing achieves a large reduction in the sampling of the signal and its recovery is achieved by using highly nonlinear methods.

Let's consider a signal x which is said to be sparse if and only if much of the entries in it are zeros. The benefit of having most of the zeros in the signal is that we can ignore them since there is no loss in signal components. Signal of length N exhibiting S number of non-zero entries, then N-S entries will be zero. Sparsity of percentage is given by %sparsity = (N-S)/N*100. The sparse signal can be reconstructed from the compressive measurements with the help of the greedy technique.

This paper discusses the signal acquisition difficulties in many scenarios. We are looking for incomplete signal quantities for the recovery of sparse Magnetic Resonance Images(MRIs). Wavelet transforms (WT) will be seen much like image compression algorithms. It represents much more sparsity of the signal under multiple decomposition levels than other transformation domains. It takes O(n) computations for reversing the signal to its original form. We can re-form the image to its original level if all wavelet sub-bands are roughly sparse [40].

2. PROBLEM STATEMENT WITH COMPRESSED SENSING.

Compressed sensing is a new platform for acquiring signals. CS involves two unique things namely Sparsity and Incoherence which involve three important aspects such as sparse representation, measurement matrix and signal recovery via Compressed Sensing technique.

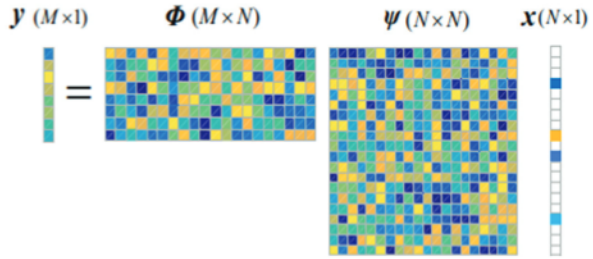

Fig. 1. Representation of Compressed Sensing model for s = 4 number of samples.

Figure 1 describes the block diagram for the CS technique where x be the input signal which is sparse in nature. The sparsity can also be achieved by making use of the transform domain. The sparsification of the image is projected onto the measurement matrix Ψ. The measurement matrix is obtained from the randn() in MATLAB 2020, where n in randn() denotes Normal Gaussian Distribution for random value generation. Consider a signal f € RN which is sparse in some domain Ψ which can be transformed by an NXN matrix Ψ = {Ψ1, Ψ2, Ψ3 - - - ΨN}. Set Ψ is the orthonormal vector bases and X be the coefficient sequence.

$$f = \sum_{i=1}^{N} \psi i x i \quad (1)$$

$$f = \Psi X \quad (2)$$

$$y = Af + e = A \Psi X + e \quad \text{Replace f by (2)} \quad (3)$$

Here y is called as measurement vector of size M, A is measurement matrix M X N and f is K-sparse signal of size N. K represent the total number of nonzero elements of signal f provided K<<M<<N. For Example, measurement matrix A can be an identity matrix, scalar matrix, random matrix or deterministic measurement. e is a noise Vector.

3. TRANSFORMATION DOMAINS

There are so many transform domains that transform the domain of the signal from one domain to another, say for example, from a frequency domain to a special domain. The Discrete Cosine Transforms (DCT) [23, 24, 26], Fast Fourier Transforms (FFT) [25] and Discrete Wavelet Transforms (DWT) [27, 28] are among the some of the transform domains. The idea behind these transformations is that we can approximate the signal in terms of its coefficients. The coefficients are in the form of low significant components and high significant components. The low significant components are the smooth areas of the image and the high significant components are the abrupt areas of the image. Low significant components hold much information about the signal/image and are highly required. These are called low-frequency components. The high significant components are less significant, less required and finally discarded. In the case of FFT, the low-frequency components are existing at 4 different corners of the image and their concertation

diminishes towards the center of the image consisting of high-frequency components. FFT is described by the phase and magnitude of the signal. FFT brings about energy compaction. In DCT, they are existing only at the upper left corner of the image and their concentration diminished towards the other three corners of the image. While in the case of DWT, it brings the transformation into 4 different sub-bands. They are High High (HH), High Low (HL), Low High (LH) & Low Low (LL). The LL components none other than our low-frequency components are exhibiting much information about the image. Wavelet transforms are used to identify both frequency and special components of the signal. Therefore, wavelet transformation is called multiresolution analysis. It is also called the next version of the Short Term Fourier Transformation (STFT). In a wavelet, the window itself is used as a wavelet. Here the window can be moved and can also be scaled. In wavelet, two types of windows are available namely wavelet window (wavelet function (ψ)) and scaling window (scaling function (Φ)).

DCT [24] and it's inverse of the equation for a 2D input signal f (x, y) is shown below by equations (4) and (5) respectively.

$$D(i,j) = 1/\sqrt{2N}(C[i]C[j]\sum_{x=0}^{M-1}\sum_{y=0}^{N-1} p(x,y)\cos\left[\frac{(2x+1)i\pi}{2N}\right]\cos\left[\frac{(2y+1)i\pi}{2N}\right] \quad (4)$$

$$f(i,j) = {}^{2}/_{N}\sum_{u=0}^{N-1}\sum_{v=0}^{N-1} C(u),C(v),F(u,v)\cos\left[\frac{(2x+1)i\pi}{2N}\right]\cos\left[\frac{(2y+1)i\pi}{2N}\right] \quad (5)$$

where C(u) = C(v) = 1/√ (2)) for u, v = 0. Otherwise, C(u) = C(v) = 1. p (x, y) is the element in the image represented by the matrix of size M X N. DCT is applied on block size N. F(u, v) is the transformed Image of f(x, y). In DCT, sine components are put in intact. The inverse of DCT is used for converting the transformed signal D(i,j) into the original signal f(i, j).

FFT [33] and its inverse are given by the following equations (6) add (7) respectively.

$$F(\omega) = \int_{-\infty}^{\infty} f(x)e^{-i\omega x}dx \quad (6)$$

$$f(x) = 1/2\pi \int_{-\infty}^{\infty} F(\omega)e^{i\omega x}d\omega \quad (7)$$

Where i= √(-1), e^iω=sin(ω)+i cos(ω). F(ω) is the FFT transformed signal, ω is the frequency and f(x) denotes the input image and x represents the time. The inverse of FFT is used for converting the transformed signal into the original signal.

The Wavelet transforms [34,35] is given by the following equation as follows.

$$F_{HighPass}(m,n) = \int_{-\infty}^{\infty} f(x)\Psi^{*}_{(m,n)}(t)dt \quad (8)$$

$$F_{LowPass}(m,n) = \int_{-\infty}^{\infty} f(x)\Phi^{*}_{(m,n)}(t)dt \quad (9)$$

$F_{HighPass}(m,n)$ represents the high pass filter to pass through high-frequency components and $F_{LowPass}(m,n)$ represents the low pass filter to pass through low-frequency components. * is the conjugate symbol. 'Ψ' represents the wavelet function given by equation (8) and 'Φ' represents the scaling function given by equation (9). The input signal is represented by f(x).

4. RELATED WORK

There are several reconstruction algorithms based on Compressed Sensing [20]. One among the CS Techniques is Orthogonal Matching Pursuit (OMP) which is a greedy or iterative method for solving compressed sensing problems. The greedy algorithm provides some sort of iterative estimation of the signal coefficients until a halting criterion met. The greedy algorithms provide performance guarantees when analyzed with convex optimization techniques [8]. OMP and *Iterative Thresholding* are the older methods of greedy approaches. OMP [9] starts by identifying the column of A correlated with the measurement matrix. This step is repeated in the algorithm by correlating the column with signal residuals. These signals are obtained by taking away the partial estimates of the signal from the original measurement vector. The stopping criterion is the number of iterations that limit the total number of nonzero in input signal f, such that y=Af. Where A is the measurement matrix. Iterative Thresholding [10] is a direct method. The signal is initially estimated as f'=0. The gradient descent step is iterated followed by hard thresholding till a stopping criterion happens.

The objective quality analysis for the reconstruction is calculated and verified by using SSIM (Structural Similarity index), PSNR (Peak Signal Noise Ratio), and RMSE (Root Mean Square Error).

The PSNR [29] is given by the equation (10),

$$\mathrm{PSNR} = 20\log(\max(f)/\sqrt{(\mathrm{MSE})}) \quad (10)$$

where f is the maximum signal component of the 2-dimensional signal.

MSE [30] is nothing but the Mean Squared Error which is given equation (11),

$$\mathrm{MSE} = (1/(m*n))\ *\mathrm{sum}(\mathrm{sum}((f-g).\ \hat{}\ 2)) \quad (11)$$

Here m and n are dimensions of the 2D signal. f is the estimated signal and g is called an actual signal.

RMSE [31] is given by equation (12),

$$\mathrm{RMSE} = \sqrt{((\mathrm{sum}\ (y`-y)2))/2)} \quad (12)$$

where y is the estimated signal and y is the actual signal.

Finally, SSIM [30] is given by equation (13),

$$\mathrm{SSIM}(a,b) = [l(a,b)]p\ .\ [c(a,b)]q\ .\ [s(a,b)]r \quad (13)$$

Here $l(a,b)=(2\mu_a\mu_b+C_1)/(\mu_a^2+\mu_b^2+C_1)$, $c(a,b)=(2\sigma_a\sigma_b+C_2)/(\sigma_a^2+\sigma_b^2+C_2)$, $s(a,b)=(\sigma_{ab}+C_3)/(\sigma_a\sigma_b+C_3)$.

Here where μ_a, μ_b, σ_a, σ_b, and σ_{ab} are the means, standard deviations, and cross-covariance for 2 dimensional signals a, b. If p = q = r = 1 (the default for Exponents), C_1 and C_2 are constants and $C_3 = C_2/2$.

5. COSAMP

The CoSaMP [32, 35] is a Compressed Sensing Technique based on OMP. It should accept the following conditions.

1. It should proceed with a minimum number of samples.
2. It should proceed by considering the samples from all different sampling schemes.
3. It should accept all the samples that are amalgamated with the noise and should be robust.

5.1 ORTHONORMAL BASES

Let consider a set B. B is having a set of vectors i.e B = $\{v_1, v_2, \ldots\ldots v_k\}$ and each of these vectors have the length 1. $\|vi\|=1$for i=1,2, …k. or $\|vi\|^2 = 1$ or $v_i \cdot v_i = 1$ for i = 1,2,3……k. All these vectors in B have magnitude or length 1 i.e. they are normalized and are unit vectors. The dot product of any two vectors in the set is 0 i.e. $v_i \cdot v_j = 0$ for i≠j. All of these vectors are orthogonal to each other.

$$\text{So } v_i . v_j = \begin{cases} 0 \text{ for } i \neq j \\ 1 \text{ for } i = j \end{cases}$$

All of these sets have magnitude or length 1 and are orthogonal to each other. They are normalized and orthogonal. So the set B is called as an orthonormal set. Ortho means every member of the set is orthogonal and everything is normalized. If there is some subspace V,

V=span(v_1, v_2, v_3, …….v_k), then B is an orthonormal basis for V. CoSaMP has received broad attention in these days due to one of Compressed Sensing technique. The CoSaMP algorithm accepts a vector of K-sparse signal.

a. It should accept the measurement matrix.
b. It should also accept the stopping criterion as the number of iterations increases, the signal quality diminishes and this is identified as the stopping criterion.

The CoSaMP is a greedy matching pursuit algorithm. Let A be the m X N sampler matrix with constant Restricted Isometry Constant (RIC) $\delta 2_s <= c$ [3]. RIC characterizes matrices which are appearing to be orthonormal and are extensively used in the field of compressed sensing. Let y=Af + e be the observed vector of samples with arbitrary signals of K-sparse amalgamated with e noise. With precision parameter έ, CoSaMP produces k-sparse estimation that is fulfilled by the equation (14).

$$\|\mathbf{f}-\mathbf{a}\|_2 <= C.\max\{\acute{\varepsilon}, 1/\sqrt{(s)}\|\mathbf{f}-\mathbf{f}_{s/2}\|_1+\|\mathbf{e}\|_2$$

Here, $f_{s/2}$ is the $(_{s/2})$ sparse estimate to f. The running time $O(\omega .\log(\|f\|_2 / \acute{\varepsilon}))$ where ω bounds the cost of the matrix vector multiplied with A. $\|f\|_2$ is l_2 normalization. c<1 and C>1 are whole constants. CoSaMP algorithm is given below.

5.2 CoSAMP: ALGORITHM

Input: A, y, s (k-sparse signal), where y= Af+e, K non-sparse signal components and e is the noise.

Output: f``: k sparse approximation of f.

Variable initialization : let $f_0 \leftarrow 0$, $y_0 \leftarrow y$, $t \leftarrow 0$

Condition: while stopping criterion does not hold, do

1. Increment the number of repetitions: $t \leftarrow t + 1$
2. Compute an intermediates: $\delta \leftarrow A^* y0$
3. Identify the main substitutions: $B \leftarrow \sup p(\delta_{2s})$
4. Support merger:$Bt \leftarrow B \cup \sup p(f^{t-1})$
5. Signal estimation by least squares: $^{b}|B^t \leftarrow (A_T^t)+B^{tb}|B^c \leftarrow 0$
6. Prune to obtain the next estimation: $f^t \leftarrow b_k$
7. Update the samples:$y_0 \leftarrow y - Af^t$

End while

$f` \leftarrow f^t$

6. PROPOSED METHODS

The proposed CoSaMP based methods for the reconstruction of Magnetic Resonance Images (MRI) include FFT based CoSaMP (FFT_CoSaMP), DFT based CoSaMP (DCT_CoSaMP) and DWT based CoSaMP (DWT_ CoSaMP). The analysis, experimentation and comparative study of these proposed methods have been done in section 6.1 below.

6.1 EXPERIMENTATION AND ITS RESULTS

The comparative study of different compressed sensing techniques is done with the Proposed techniques. Our proposed techniques are giving good results compared to other techniques as depicted in table 1, table 2 and table 3 for PSNR, SSIM and RMSE respectively. The PSNR value of the proposed methods would be like FFT_CoSaMP of 36.01, DCT_CoSaMP of 36.33 and DWT_CoSaMP of 37.16 (db4), 36.12(coif3) and 38.5 (Sym8) for a measurement matrix of 210 X 256 of input image size of 256 X 256 as in table 1. These PSNR values are validating that our proposed DWT_CoSaMP method is the best compared to other methods. Similarly, SSIM value 0.81 of the proposed method DWT_ CoSaMP is better as compared to other CS Based techniques like FFT_CoSaMP of 0.7, DCT_CoSaMP of 0.73 and other methods of CS as in table 2. In Case of DWT_ CoSaMP, the SSIM value for Coif3 is 0.68, for db4 of 0.71 and for haar of 0.81 for a measurement matrix of 210 X 256 of the input image size of 256 X 256. In the same way, RMSE value of the proposed method DWT_CoS-

aMP 0.44 achieves good results when compared to other CS-based techniques like FFT_CoSaMP is 0.66, DCT_CoSaMP is 0.55 and other methods as shown in table 3.

The System Requirements for conduction of simulation experiment on CoSaMP based CS technique will consist of system of Windows 10 Operating System, secondary memory of 500GB, 2.2 GHz speed, RAM is 6 GB, and MATLAB software 2020.

Table 1. PSNR based comparison for CoSaMP named Compressed Sensing technique

Sl. No.	References	Method	PSNR
1	Improved CoSaMP Reconstruction Algorithm Based on Residual Update[12]	COSaMP	25.93
2	A Study on Image Reconfiguration Algorithm of Compressed Sensing [13]	St.OMP	28.3
3	Adaptive gradient-based block compressive sensing with sparsity for noisy images [14]	AGbBCS SP	23..73
4	Variable atomic number MP for Image restoration [15]	CoSaMP	35.5875
5	An Improved Off-Grid Algorithm Based on CoSaMP for ISAR Imaging[[35]	CoSaMP	30.01
6	Constrained Backtracking Matching Pursuit Algorithm for Image Reconstruction in Compressed Sensing[36]	CBMP	34.04
7	Proposed method	FFT_CoSaMP	36.01
		DCT_CoSaMP	36.33
		DWT_CoSaMP	37.16 (DB4)
			38.12 (Coif3)
			38.5 (Sym8)

Table 1 depicts the comparison of PSNR values that were experimented with some research articles under different Compressed Sensing techniques. Among all the references, the proposed methods FFT_CoSaMP, DCT_CoSaMP and DWT_CoSaMP achieve better PSNR results concerning referenced results.

Similarly, Table 2 illustrates the comparison of SSIM values that were experimented with some other research articles under different compressed sensing techniques. Among all the references, the proposed method FFT_CoSaMP, DCT_CoSaMP and DWT_CoSaMP give the best SSIM results concerning referenced results.

In the same way, Table 3 demonstrates the comparison of RMSE values that were experimented with various research articles under different compressed Sensing techniques. Among all these references, the proposed method FFT_CoSaMP, DCT_CoSaMP and DWT_CoSaMP give good results concerning referenced results.

Table 2. SSIM based comparison for CoSaMP named Compressed Sensing technique

Sl. No.	References	Method	SSIM
1	Diffuse optical tomography image reconstruction via greedy algorithm [16]	CoSaMP	0.5443
2	Quantitative Comparison Of Reconstruction Methods For Compressive Sensing MRI [37]	CoSaMP	0.8
3	Recovery from compressed measurements using Sparsity Independent Regularized Pursuit, Signal Processing[38]	SIRP	0.75
4	Sparse recovery based compressive sensing algorithms for diffuse optical tomography[17]	CoSaMP	0.74
5	CS-based MRI image reconstruction via quantitative Comparison [18]	CoSaMP	0.79
6	DCT based CS recovery Strategies' in medical imaging[19]	DCT based Method	0.80
7	Proposed method	FFT_CoSaMP	0.7
		DCT_CoSaMP	0.73
		DWT_CoSaMP	0.81

Table 3. RMSE based comparison for CoSaMP named Compressed Sensing technique

Sl. No.	References	Method	RMSE
1	A novel compressive sampling method for ECG wearable measurement systems[39]	DBBD +DCT	3.8
2	Sparse Reconstruction Off-grid OFDM Time Delay Estimation Algorithm Based on Bayesian Automatic Relevance Determination[21]	FFT Expectation maximization (EM) algorithm	3.1
3	An improved statistical iterative algorithm for sparse-view and limited-angle CT image reconstruction [22]	Median and Wiener filtering algorithms	0.91
4	Proposed method	FFT_CoSaMP	0.66
		DCT_CoSaMP	0.55
		DWT_CoSaMP	0.44

Table 4 shows the analysis of various measurement matrices for the Thorax MRI image reconstruction. The measurement matrices of higher dimensions give comparatively worthy results than the lower dimensions of the measurement matrix. Here the dimensions 210X256 are the best measurement matrix for our experimental simulations. For the measurement matrix 210 x 256, DFT based CoSaMP gives PSNR of 54.95, SSIM of 0.69 and RMSE of 0.45. For the same 210 X 256 measurement matrix, the FFT-based CoSaMP gives the PSNR of 52.5, SSIM of 0.66 and RMSE of 0.45. But in the case of

DWT-based CoSaMP, for the same measurement matrix of 210 XX 256, PSNR is 57.63, SSIM is 0.71 and RMSE is 0.33. Under different wavelet families, DWT-based CoSaMP with db4, haar, sym8, and coif3 gives the PSNR values 54.16, 53.12, 55.18, and 55.12 respectively.

Table 4. Analysis of measurement matrix for MRI image reconstruction for the thorax image.

CS Technique for Thorax	Measurement matrix	PSNR	SSIM	RMSE
DCT based CoSaMP	5 X 256	27.1	0.05	11.25
	30X256	35	0.13	4.75
	55X256	37.12	0.21	3.52
	80X256	40.1	0.29	2.82
	105X256	42.23	0.37	1.6
	130X256	46.23	0.46	1.75
	155X256	47.8	0.54	1.02
	180X256	50.23	0.6	0.75
	210X256	54.95	0.69	0.45
FFT based CoSaMP	5 X 256	27.2	0.1	10
	30X256	33.62	0.15	3.52
	55X256	38.12	0.286	2.13
	80X256	42.67	0.39	1.75
	105X256	44.12	0.47	1.62
	130X256	46.2	0.52	1.52
	155X256	47.5	0.56	1.23
	180X256	48.6	0.59	0.75
	210X256	52.5	0.66	0.45
DWT based CoSaMP	5 X 256	24.5	0.02	15.75
	30X256	26.8	0.12	11.53
	55X256	32.1	0.24	6.89
	80X256	42.9	0.38	1.98
	105X256	46.23	0.48	2.05
	130X256	49.1	0.56	1.12
	155X256	51.1	0.59	0.89
	180X256	52.8	0.36	0.52
	210X256	57.63	0.71	0.33
	210 X 256	db4 54.16	-	-
		haar 53.12	-	-
		sym 55.18	-	-
		coif3 55.12	-	-

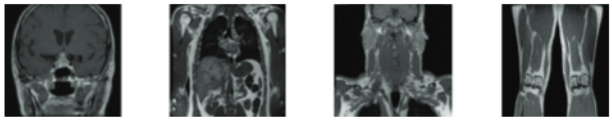

Fig. 2. MRI images of a) Brain, b) Lungs c) Thorax d) Thighs

Figure 2 shows different MRI images like a) Brain, b) Lungs c) Thorax d) Thighs The experiential results are tabulated above for the measurement matrix of 210 X 256. The tabulated values show the better reconstruction and analysis of MRI images. The average values at the bottom of the table 5 for PSNR, SSIM and RMSE give the better analysis and approximation and reconstruction of the image. And figure 3 shows the simulated graphs of PSNR, SSIM, RMSE values against different measurement matrices of Table 4.

In our experimental work, about 250 MRI images are used for experimentation by making use of a measurement matrix of 256 X 210. Among 250 images, 35 images are filtered and discussed in this research work. The below tabulation shows the statistical values of the FFT_CoSaMP, DCT_CoSaMP, and DWT_CoSaMP. The images used for experimentation are of some cancerous and non-cancerous human brain MRI images. The cancerous images are named as Yes and non-cancerous images are named as No.

Other than human brain images, we have used some of the other MRI images of human lungs, Thighs, and Thorax. The outcome for these images concerning their PSNR, PSNR, SSIM, and RMSE are tabulated in Table 5. Here the thorax MRI image is giving good results concerning PSNR, SSIM and RMSE values when compared to other MRI images. And also the average values for the same are computed, tabulated and compared as in Table 5.

Table 5. The proposed CS Techniques FFT_ CoSaMP, DCT_CoSaMP, DWT_ CoSaMP have been experimented with for 250 images and only 35 images are shown in the table images of Brain, Lungs, Thorax and Legs.

Sl. No.	MRI Image No- NonCancerous Yes-Cancerous	PSNR FFT_ CoSaMP	PSNR DCT_ CoSaMP	PSNR DWT_ CoSaMP
1	No 1	28.97	30.02	32.83
2	No 2	26.34	27.27	32.54
3	No 3	22.86	24.57	32.91
4	No 4	30.96	31.86	36.12
5	No 5	27.1	27.92	33.15
6	No 6	24.53	25.4	29.41
7	No 7	33.29	34.27	36.27
8	No 8	33.3	34.25	36.28
9	No 9	30.33	31.57	39.72
10	No 10	30.4	32.03	36.99
11	No 11	30.09	32.6	36.87
12	No 12	23.27	24.85	29.19
13	No 13	25.76	28.81	31.59
14	No 14	25.78	27.18	34.18
15	No 15	25.46	26.89	33.27
16	No 16	27.06	28.07	33.33
17	No17	20.28	22.54	29.47
18	No 18	27.45	28.61	32.25
19	No 19	26.05	27.21	29.36
20	No 20	23.24	24.88	28.44
21	No 21	29.16	31.03	33.89
22	No 22	23.59	24.63	28.14
23	No 23	26.02	27.18	30.68
24	No 24	25.81	27.08	34.1
25	No 25	26.41	29.1	33.04
26	No 38	24.74	25.26	38.42
27	No 94	28.2	29.07	37.49

28	No 95	28.88	31.44	39.66
29	No 96	29	30.64	38.35
30	Yes 102	28.08	28.36	37.26
31	Yes 103	28.28	29.35	32.9
32	Yes 128	32.58	34.44	37.67
33	Lungs	30.87	32.96	34.01
34	Thighs	34.71	36.86	40.1
35	Thorax	55.46	55.02	57.62
	Average	**28.98**	**30.02**	**34.72**

Sl. No.	MRI Image No- NonCancerous Yes-Cancerous	SSIM		
		FFT_ CoSaMP	DCT_ CoSaMP	DWT_ CoSaMP
1	No 1	0.5	0.5	0.67
2	No 2	0.45	0.44	0.58
3	No 3	0.34	0.35	0.51
4	No 4	0.38	0.38	0.6
5	No 5	0.42	0.41	0.51
6	No 6	0.45	0.45	0.58
7	No 7	0.6	0.6	0.65
8	No 8	0.6	0.6	0.65
9	No 9	0.25	0.25	0.53
10	No 10	0.34	0.34	0.49
11	No 11	0.35	0.37	0.6
12	No 12	0.46	0.47	0.57
13	No 13	0.62	0.65	0.71
14	No 14	0.45	0.45	0.57
15	No 15	0.38	0.39	0.47
16	No 16	0.39	0.38	0.5
17	No17	0.47	0.49	0.01
18	No 18	0.42	0.43	0.64
19	No 19	0.51	0.54	0.57
20	No 20	0.59	0.61	0.7
21	No 21	0.59	0.61	0.52
22	No 22	0.42	0.43	0.54
23	No 23	0.62	0.63	0.73
24	No 24	0.45	0.45	0.57
25	No 25	0.6	0.62	0.71
26	No 38	0.42	0.4	0.73
27	No 94	0.34	0.33	0.58
28	No 95	0.32	0.33	0.5
29	No 96	0.36	0.36	0.56
30	Yes 102	0.62	0.54	0.83
31	Yes 103	0.66	0.66	0.73
32	Yes 128	0.7	0.7	0.8
33	Lungs	0.76	0.79	0.81
34	Thighs	0.56	0.57	0.59
35	Thorax	0.66	0.69	0.71
	Average	**0.487**	**0.5**	**0.59**

Sl. No.	MRI Image No- NonCancerous Yes-Cancerous	RMSE		
		FFT_ CoSaMP	DCT_ CoSaMP	DWT_ CoSaMP
1	No 1	7.91	6.92	5.17
2	No 2	6.34	6.75	4.26
3	No 3	9.43	4.63	3.82
4	No 4	5.41	6.59	4.3
5	No 5	7.26	5.51	4.23
6	No 6	6.72	6.89	5.3
7	No 7	6.32	5.23	4.7
8	No 8	8.31	7.32	5.39
9	No 9	6.82	6.81	2.63
10	No 10	6.52	6.31	3.91
11	No 11	7.23	5.5	5.01
12	No 12	9.51	7.29	3.71
13	No 13	8.72	9.23	6.88
14	No 14	6.32	6.23	3.96
15	No 15	6.23	7.21	4.26
16	No 16	7.12	8.61	5.23
17	No17	8.56	7.69	4.28
18	No 18	7.26	6.23	5.36
19	No 19	7.12	6.23	2.35
20	No 20	5.63	5.64	4.32
21	No 21	9.23	7.25	4.5
22	No 22	7.91	6.29	5.23
23	No 23	7.23	5.23	3.85
24	No 24	9.63	7.63	6.32
25	No 25	7.52	4.23	3.25
26	No 38	6.85	5.98	4.35
27	No 94	6.35	3.54	3.54
28	No 95	7.51	6.81	2.6
29	No 96	6.32	6.23	4.65
30	Yes 102	10.71	6.6	3.5
31	Yes 103	7.98	6.25	5.91
32	Yes 128	4.91	4.81	3.21
33	Lungs	6.44	6.44	5.12
34	Thighs	2.5	2.5	2.5
35	Thorax	0.45	0.45	0.33
	Average	**7.38**	**6.31**	**4.29**

Table 6. The CoSaMP based CS technique along with Different types of dictionaries like DFT, FFT and DWT have experimented for four different images of the Brain, Lungs, Thorax and Legs.

MRI image	Proposed Method	PSNR	SSIM	RMSE
Brain	FFT_CoSaMP	31.2	0.698	4.52
	DCT_CoSaMP	33.2	0.623	6.20
	DWT_CoSaMP	36.6	0.754	4.83
Lungs	FFT_CoSaMP	30.87	0.754	6.44
	DCT_CoSaMP	32.96	0.787	6.44
	DWT_CoSaMP	34.2	0.808	5.12
Thorax	FFT_CoSaMP	52.5	0.665	0.66
	DCT_CoSaMP	54.95	0.646	0.66
	DWT_CoSaMP	57.63	0.665	0.44
Thighs	FFT_CoSaMP	34.7	0.56	3.75
	DCT_CoSaMP	36.76	0.57	3.76
	DWT_CoSaMP	40.26	0.58	2.475

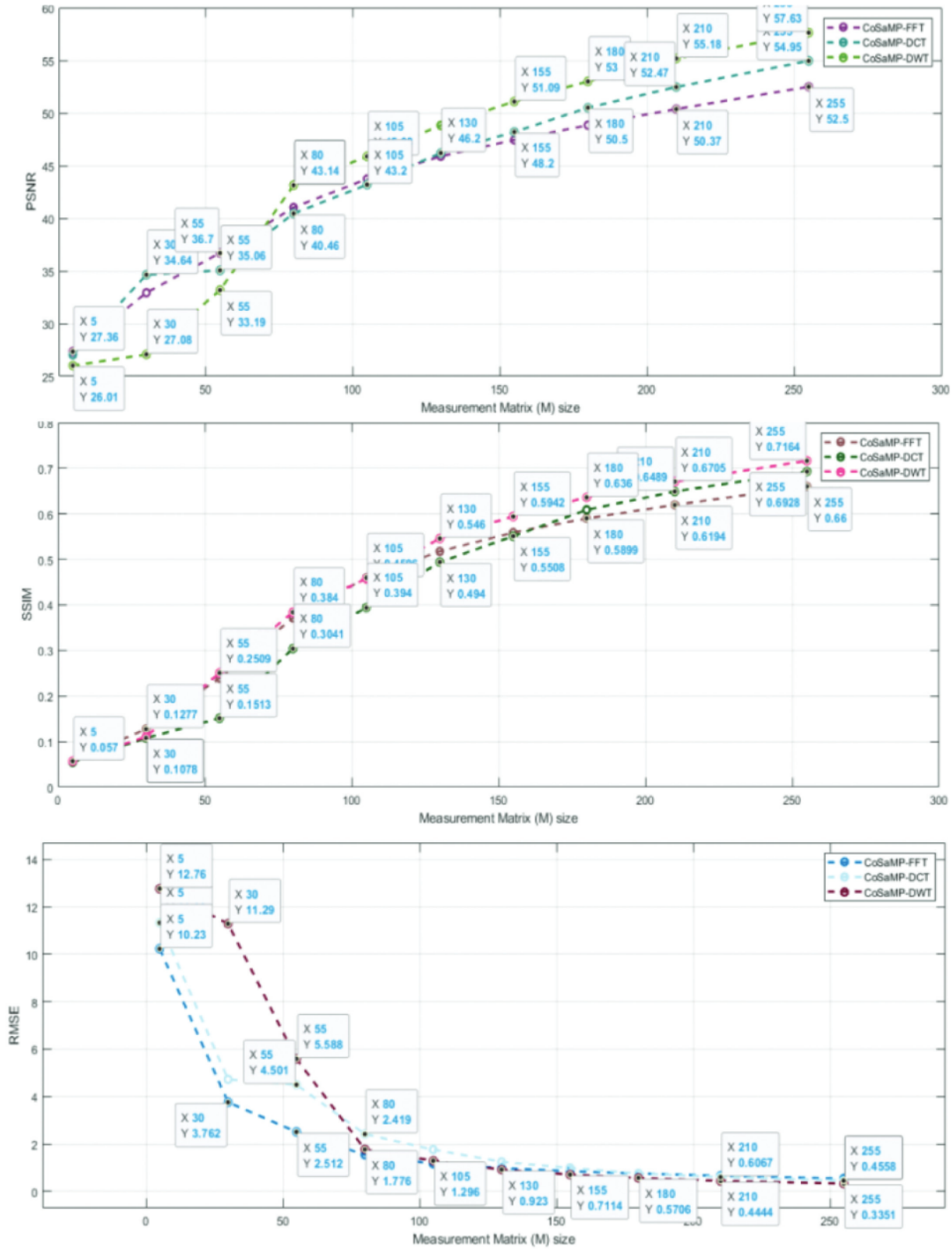

Fig. 3. PSNR, SSIM and RMSE based Simulated Graphs for the reconstruction of Thorax Image.

7. CONCLUSION AND FUTURE ENHANCEMENT

For restoration of MRI images, based on different traditional methods and proposed Compressed Sensing methods such as FFT_CoSaMP, DCT_CoSaMP and DWT_CoSaMP, DWT_CoSaMP is giving best results concerning SSIM, RMSE and PSNR statistical values. When DWT_CoSaMP is passed with different dictionaries of Wavelets families like coif3, db4 haar and sym8, the result is said to be likely good for all the families of wavelet transforms. For Further future scope, CS-based methods of reconstruction will be applied for the investigation of music and speech signals by making use of different types of sparse dictionary parameters.

8. ACKNOWLEDGMENT

I would like to thank Visvesvaraya Technological University (VTU), Gnana Sangama, Belagavi - 590018, Karnataka, India for the monetary support extended to my research work.

9. REFERENCES:

[1] D. L. Donoho, "Compressed sensing", IEEE Transactions on Information Theory, Vol. 52, No. 4, 2006, pp. 1289-1306.

[2] G. Yang et al. "DAGAN: deep de-aliasing generative adversarial networks for fast compressed sensing MRI reconstruction," IEEE Transactions on Medical Imaging, Vol. 37, No. 6, 2018, pp. 1310-1321.

[3] Y. Zhang B. P. Wang Y. Fang, Z. X. Song, "SAR Observation Error Estimation Based on Maximum Relative Projection Matching", International Journal of Antennas and Propagation, 2020.

[4] D. L. Donoho, "Compressed sensing", IEEE Transactions on Information Theory, Vol. 52, 2006, pp. 1289-1306.

[5] M.B Cand'es, E. J. Wakin, "An Introduction to Compressive Sampling", Signal Processing Magazine IEEE, Vol.2, No. 5, 2008.

[6] E. Candes, J. Romberg, "Sparsity and incoherence in compressive sampling", Inverse Problems, Vol.23, 2007, p. 969.

[7] E. Candes, J. Romberg, T. Tao, "Robust uncertainty principles: Exact signal reconstruction from highly incomplete frequency information", IEEE Transactions on Information Theory, Vol.52, No.2, 2006, p. 489.

[8] M. Lustig, D. Donoho, John M. Pauly. "Sparse MRI: The Application of Compressed Sensing for Rapid MR Imaging", Magnetic Resonance in Medicine, 2007, pp. 1182 1195.

[9] S. Mallat, Z. Zhang. "Matching pursuits with time-frequency dictionaries", IEEE Transactions on Signal Processing, Vol. 41, No. 12, 1993, pp. 3397-3415.

[10] M. Elad, B. Matalon, J. Shtok, M. Zibulevsky. "A wide-angle view at iterated shrinkage algorithms", Proceedings of the SPIE Optics Photonics: Wavelets, San Diego, CA, USA, August 2007.

[11] H. J. Landau", Sampling, data transmission, and the Nyquist rate", Proceedings of the IEEE, Vol. 55, No. 10, 1967, pp. 1701-1706.

[12] D. Lu, G. Sun, Z. Li, S. Wang, "Improved CoSaMP Reconstruction Algorithm Based on Residual Update" Journal of Computer and Communications", Scientific research publishing, Vol.7 No.6, 2019.

[13] Y. Zhang, D. Wang, L. Kan, P. Zhao, "A Study on Image Reconfiguration Algorithm of Compressed Sensing", TELKOMNIKA, Vol.15, No.1, 2017, pp. 299-305.

[14] H.-H. Zhao, P. L. Rosin, Y.Lai, J. Zheng, Yao-Nan Wang, "Adaptive gradient-based block compressive sensing with sparsity for noisy images", Multimedia Tools and Applications, Vol. 79, 2019, pp. 14825-14847.

[15] H. Zhao, C. Chen, C. Shi, "Image reconstruction algorithm based on variable atomic number matching pursuit", Journal of Algorithms & Computational Technology, Vol. 11, No. 2, 2017, pp. 103-109.

[16] B. P. V. Dileep, T. Das, K. Dutta "Greedy algorithms for diffuse optical tomography reconstruction", Optics Communications, Vol. 410, No. 1, 2018, pp. 164-173.

[17] B. P. V. Dileep, T. Das, K. Dutta, "Sparse recovery based compressive sensing algorithms for diffuse optical tomography", Optics & Laser Technology, Vol. 128, 2020.

[18] T. S. Kavita, K. S. Prasad, "Quantitative Comparison of Reconstruction Methods for Compressive Sensing MRI", International Journal Of Scientific & Technology Research Vol. 8, No. 10, 2019.

[19] Amira S, Ashour Yanhui Guo, Eman Elsaid Alaa, Hossam M.Kasem, "Discrete cosine transform based compressive sensing recovery strategies in medical imaging", Advances in Computational Techniques for Biomedical Image Analysis, Academic Press, 2020.

[20] R. Zhang, C. Meng, C. Wang, Q. Wang, "Compressed Sensing Reconstruction of Radar Echo Signal Based on Fractional Fourier Transform and Improved Fast Iterative Shrinkage-Thresholding Algorithm" Wireless Communications and Mobile Computing, 2021.

[21] P. Zhang, B. Ba, Y. Zhang, P. Han, "Sparse Reconstruction Off-grid OFDM Time Delay Estimation Algorithm Based on Bayesian Automatic Relevance Determination", Journal of Physics: Conference Series, Vol. 1237, No. 2, 2019.

[22] Z. Hu et al. "An improved statistical iterative algorithm for sparse-view and limited-angle CT image reconstruction". Scientific Report, Vol. 7, 2017.

[23] N. Ahmed, T. Natarajan, K. R. Rao, "Discrete cosine transform," IEEE Transactions on Computers, Vol. C-23, 1974, pp. 90-93.

[24] J. W. Cooley, P. A. W. Lewis, P. D. Welch, "The Fast Fourier Transform and Its Applications", IEEE Transactions on Education, Vol. 12, No. 1, 1969, pp. 27-34.

[25] Z. Wu; J. Sha; Z. Wang; L. Li; M. Gao, "An improved scaled DCT architecture", IEEE Transactions on Consumer Electronics, Vol. 55, No. 2, 2009, pp. 685-689.

[26] S. G. Mallat, S. Zhong, "Characterization of signals from multiscale edges", IEEE Transactions on Pattern Analysis and Machine Intelligence, Vol. 14, No. 7, 1992, pp. 710-732.

[27] A. N. Akansu, W. A. Serdijn, I. W. Selesnick, "Wavelet Transforms in Signal Processing: A Review of Emerging Applications", Physical Communication, Vol. 3, No. 1, 2010, pp. 1-18.

[28] C. A. Chalaperumal, S. D. kumar, "An Efficient Image Quality Enhancement using Wavelet Transform", Materials Today: Proceedings, Vol. 24, Part 3, 2020.

[29] V. Bruni, D. Vitulano, "An entropy-based approach for SSIM speed up", IEEE Signal Processing, Vol. 135, 2017, pp. 198-209.

[30] J. F. Kenney, E. S. Keeping, "Root Mean Square." Mathematics of Statistics, Princeton, NJ, USA, pp. 59-60, 1962.

[31] D. Needell, J. A. Tropp, "CoSaMP: Iterative signal recovery from incomplete and inaccurate samples", Applied and Computational Harmonic Analysis, Vol. 26, 2009, pp. 301-321.

[32] E. Ayanoglu, "Data transmission when the sampling frequency exceeds the Nyquist rate", IEEE Communications Letters, Vol. 1, No. 6, 1997.

[33] P. Heckbert, "Fourier Transforms and the Fast Fourier Transform (FFT) Algorithm", Computer Graphics 2, 1998.

[34] J. D. Villasenor, B. Belzer, and J. Liao "Wavelet filter evaluation for image compression", IEEE Transactions on Image Processing, Vol. 4, 1995, pp. 1053-1060.

[35] J. Cheng "An Improved Off-Grid Algorithm Based on CoSaMP for ISAR Imaging", Proceedings of the 5th International Conference on Mechanical, Control and Computer Engineering, Harbin, China, 25-27 December 2020.

[36] X. Bi, L. Leng, C. Kim, X. Liu, Y. Du, F. Liu, "Constrained Backtracking Matching Pursuit Algorithm for Image Reconstruction in Compressed Sensing". Applied Science, Vol. 11, 2021, p. 1435.

[37] T. S. Kavita, K. S. Prasad, "Quantitative Comparison of Reconstruction Methods For Compressive Sensing MRI", International Journal Of Scientific & Technology Research, Vol. 8, No. 10, 2019.

[38] T. J. Thomas, J. S. Rani, "Recovery from compressed measurements using Sparsity Independent Regularized Pursuit", Signal Processing, Vol. 172, 2020.

[39] F. Picariello, G. Iadarola, E. Balestrieri, I. Tudosa, L. De Vito, "A novel compressive sampling method for ECG wearable measurement systems", Measurement, Vol. 167, 2021.

[40] Y. Liu, X. Chen, A. Liu, R. K. Ward, Z. J. Wang, "Recent Advances in Sparse Representation Based Medical Image Fusion," IEEE Instrumentation & Measurement Magazine, Vol. 24, No. 2, 2021, pp. 45-53.